RIGIDITY AND STRENGTH OF REINFORCED CONCRETE STRUCTURE WITH SPANDRELS AND WING WALLS

by

SETSURO NOMURA* and KAZUHIDE SATO**

SYNOPSIS

The influence of the spandrels and wing walls attached to a column on its rigidity, strength and ductility are studied by the elastic-plastic FEM analysis as well as by the experiment to get more detailed data on crack increasing process and deformation ability.

THEORETICAL ANALYSIS

Analytical model and the wall sizes for FEM Analysis are shown in Fig 1 and Table 1. The walls and other members are divided to rectangular elements, where the size of the column elements are decided so as to get a fine stress distribution. The characteristics of the materials are shown in Table 2. Buckling and slippage of the reinforcing bar are not considered and the bar is treated as a line element. A horizontal force is distributively applied to each beam element according to its area. The equilibrium for the load increment in plastic range is decided by an interaction method using the equivalent stiffness and the strain energy increment.

From the figures of the stress distribution to bending moment and shear force, the stress concentration at the corners of the openings and the deformable zone into the spandrels are noticed. The initial rigidity Ki derived from FEM is shown in Fig 3. The value of Ki increases with the increase of wall elements. Under the same opening length ratio ξ ($\xi = \sqrt{h_o l_o / h' l'}$), the wing walls influence on the rigidity more than spandrel walls.(Fig 3)

Fig 2 shows the $p - \delta$ curves to monotonic increasing load where the displacement at the maximum load is not certain because of the load incremental method used in this paper. The wider are the widths of wing walls and spandrels the higher maximum loads are given. Especially the influences of wing walls are great. In case of wing walls, this increase of maximum load to bending moment is caused by the vertical reinforcing bars of the wall and the increase of compression area of concrete at the column section, and to shear force it is caused by the increase of the column section area. On the other hand, spandrels lessen the shear span ratio of the column, which is the main reason to increase the maximum shear strength.

EXPERIMENTAL STUDY

As shown in Fig 4, 12 kinds of specimen are tested. Alternately repeating load is applied at the following displacement levels (three times at one level, and then increase to next level) until it is judged that the execution to further level is imposible to keep the constant column axial forces, which are in stress expression, Fc/6 and Fc/12 at center and both

---

*Associate Prof., and **Research Assistant, Dep. of Architectural Eng., Sience Univ. of Tokyo, Noda City, Japan

end columns respectively. The displacement levels are 0.5, 1, 2, 4, 6, 8, 12, 16, 20, 30, 40(x 10^{-3} rad). Fig 5 shows the examples of the load displacement curve. The results of the experiments are listed in Table 3 and compared with those of FEM and Limit Analysis, and mostly well correspondence was observed among them.

The Limit Analysis is based on the elastic-plastic matrix method considering the rigid parts in the panel zone. The length of the deformable part is assumed $l_w/2$, where l_w is the width of the member including the attached wall. The maximum sectional strength for bending moment Mu and shear force Qu are given by the following equations recommended by Ohkubo in Ref.(1).

$$Mu = (g_t+\beta_c)a_t \cdot \sigma_y \cdot D + \{g_1+0.5(\beta_c+\beta_t)\}\sum a_{tw} \cdot \sigma_{yw} \cdot D + 0.5ND\left[1+2\beta_c - \frac{N}{bDF_c}\left\{1+(1-r)\frac{a_t \cdot \sigma_y}{N}\right\}^2\right] \quad --(1)$$

$$Qu = \left\{\frac{0.115^{*} k_u \cdot k_p (180+F_c)}{M/Q \cdot d_e + 0.115} + 2.7\sqrt{p_w \cdot \sigma_{yw}\left(\frac{b}{b_e}\right) + p_{sh} \cdot \sigma_{yh}\left(\frac{t}{b_e}\right)}\right\} b_e \cdot \frac{7}{8} d_e + 0.1N \quad --(2)$$

In Eq.(2) the column with wing walls at both sides is treated as an equivalent rectangular column of the same width and area as shown in Fig 11. (Note: The value of * mark is taken as a mean value, though in Ref.(1) it is taken as a minimum value 0.092.)

Fig 6 shows the cracks at the maximum load, and it is said that the increase of the width of the spandrels makes the column shorter and in case of [F → TK1 → TK2], the breaking mode changes from bending to shear type. The column becomes more wall-like type with the increase of the width of the wing walls and in case of [F → S1 → S2 → S3], the flexural breaking of the column changes to the diagonal X type shear breaking where the shear cracks of both wing walls thrust through the center column. Two types of shear cracks are shown in Fig 6. One is the main crack lines diagonally crossing the corners of the two openings as S2, 3, STK11, 12, 21, and the other is those crack lines which do not cross the corners of the two openings as STK22, 32, 42. In case of the latter type the maximum loads given by the Limit Analysis are less than those given by the experiment. From the fact and also from the shear stress distribution after cracking given by FEM, it is considered that the length of d_e in Eq.(2) should be taken longer to these types than that taken in Ref.(1). (Fig 11)

Fig 10 shows the envelope curves, and it is observed that every curve approaches to the curve F after maximum load. The specimens where ζ is less than 0.7 reach to the maximum load at the displacement of about 4×10^{-3} rad. The equivalent viscous damping ratios derived by the steady state loop of each load level are ploted in Fig 9.

The attachment of spandrels or wing walls gives the higher bearing capacity but less ductility. A more definite design theory for the treatment of these walls should be considered.

ACKNOWLEDGMENT

The experiment was executed with the finantial support of Research Foundation of Ogawa Scholarship Society.

REFERENCE

(1) Masamichi Ohkubo, "Review on the Ultimate Strength of RC Members with Spandrels and Wing Walls", Summaries of Tech. Papers of Annual Meeting of of AIJ, Sep. 1979.

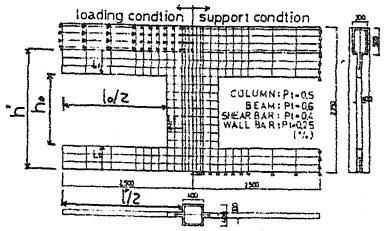

Fig. 1 Analytical Model

Table 1 Size of Models

MODEL	SPANDREL WALL UPPER L_1 (cm)	SPANDREL WALL LOWER L_3 (cm)	WING WALL L_2 (cm)
* T-000	0	0	0
* T-010	0	0	30
* T-020	0	0	60
T-030	0	0	90
T-100	45	0	0
* T-110	45	0	30
T-120	45	0	60
T-130	45	0	90
* T-200	75	0	0
* T-220	75	0	60
T-001	0	45	0
* T-101	45	45	0
* T-111	45	45	30
T-121	45	45	60
T-131	45	45	90
T-201	75	45	0
* T-102	45	75	0
* T-202	75	75	0
T-212	75	75	30
* T-222	75	75	60
T-232	75	75	90
* T-999	SHEAR WALL		

Table 2 Characteristics of Materials

concrete	
stress strain curve	Tri-Linear
compressive strength	210 kg/cm^2
tenslie strength	21 kg/cm^2
young's modulus	2.1×10^5 kg/cm^2
steel reinforcement	
stress strain curve	Bi-Linear
yield strength	3000 kg/cm^2
tensile strength	4200 kg/cm^2
young's modulus	2.1×10^6 kg/cm^2

Wall Thickness: 10 cm
Column Axial Force
* : 0 kg/cm^2 and 30 kg/cm^2
no Mark : 0 kg/cm^2

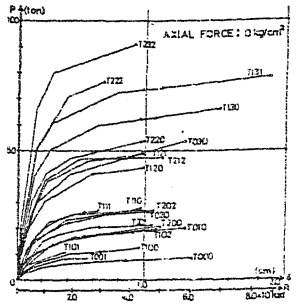

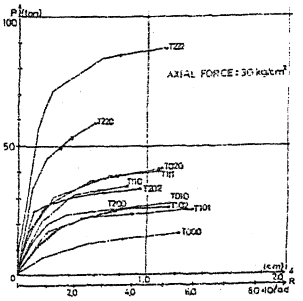

Fig. 2 Skeleton Curves

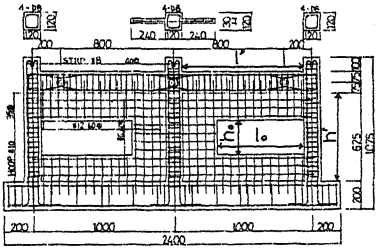

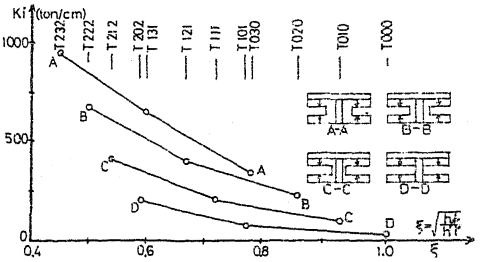

Fig. 3 Ki - ξ

SPECIMEN		F	ST1	ST2	ST3	TK1	TK2	STK11	STK21	STK12	STK22	STK32	STK42
SPANDREL WALL	UPPER (cm)	0	0	0	0	10.3	19.3	10.3	10.3	19.3	19.3	19.3	19.3
	LOWER (cm)	0	0	0	0	10.3	19.3	10.3	10.3	19.3	19.3	19.3	19.3
WING WALL (cm)		0	12	24	36	10	19.3	12	24	12	24	36	48
MAIN REINFOR-CEMENT	COLUMN	4 - D8 , P_t = 0.7 %											
	BEAM	4 - D10 , P_t = 0.5 %											
SHEAR REINFOR-CEMENT	COLUMN	#10, @35, P_w = 0.38 %											
	BEAM	#8 , @40, P_w = 0.31 %											
	WALL	#12, @ 60, P_w = 0.3 %											
WALL THICKNESS		3 cm											

Fig. 4 Details of Specimen

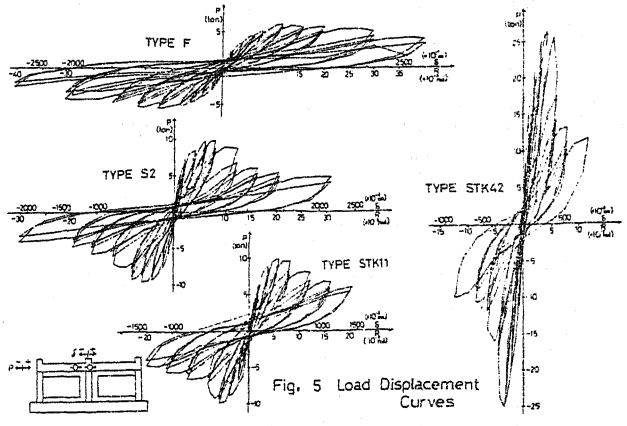

Fig. 5 Load Displacement Curves

Table 3 Results of Experiments and Analyses

SPECIMEN	INITIAL RIGIDITY (Ki) (ton/cm)			FIRST CRACKING LOAD (ton)			MAX. LOAD (Pu) (ton)		
	E.XP.	F.E.M.	LIMIT A.	E.XP.	F.E.M.	LIMIT A.	EXP.	F.E.M.	LIMIT A.
F	36.7	43.5	33.9	1.41	1.66	1.15	5.73	6.46	5.9
S1	74.6	84.3	74.0	2.12	1.67	1.56	6.87	7.69	7.8
S2	130.0	151.4	148.5	3.63	2.06	2.30	9.75	9.95	10.1
S3	206.3	235.6	244.9	5.30	2.70	3.03	11.90	12.60	12.7
TK1	60.5	69.0	74.0	1.29	1.67	1.70	7.58	8.11	7.6
TK2	137.0	158.4	173.7	2.08	1.72	2.81	8.50	11.10	9.7
STK11	124.4	143.3	112.5	3.75	1.81	1.73	9.84	10.30	9.9
STK21	209.6	231.9	209.8	3.79	2.71	2.64	12.70	12.90	13.7
STK12	o 143.0	260.7	207.9	2.15	1.87	2.70	12.00	13.30	13.3
STK22	o 202.8	365.6	308.8	4.62	3.56	3.64	16.20	17.10	15.9
STK32	o 359.0	474.9	426.2	5.74	4.58	4.99	20.40	20.00	18.9
STK42	o 503.0	598.1	558.4	5.72	5.44	6.78	25.60	26.20	22.8

o-shrinkage cracks were produced in walls before experiment

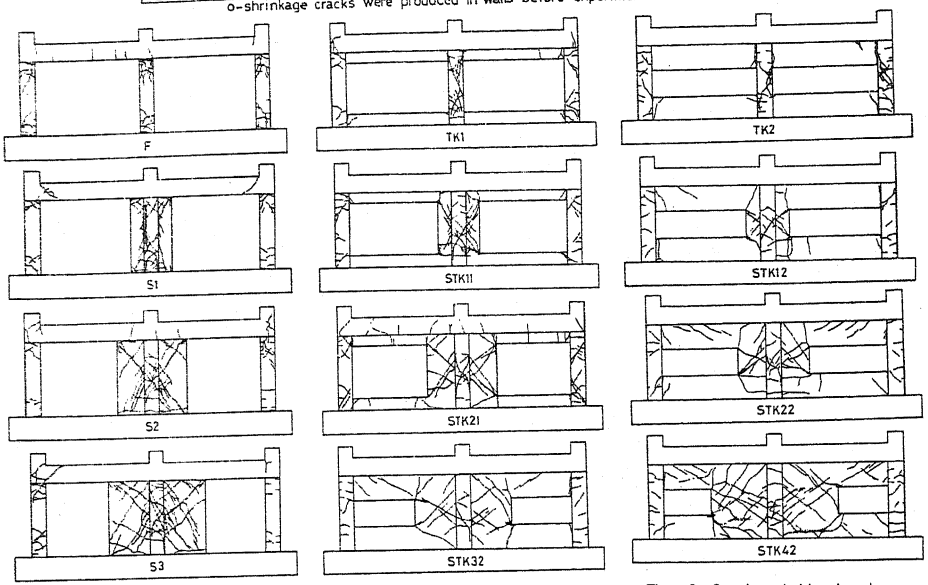

Fig. 6 Cracks at Max. Load

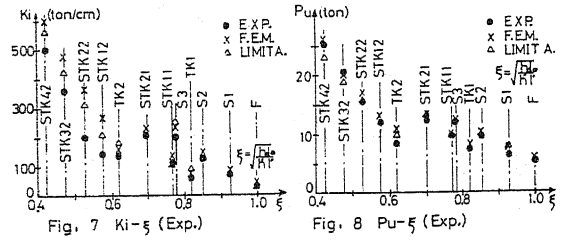

Fig. 7 Ki-ξ (Exp.)

Fig. 8 Pu-ξ (Exp.)

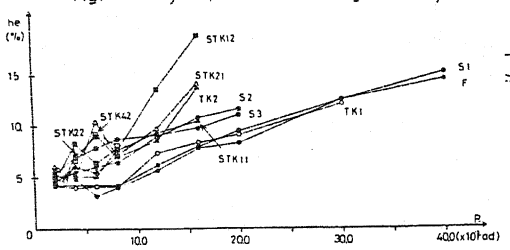

Fig. 9 Equivalent Viscous Damping Ratio

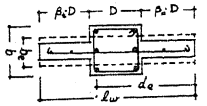

Fig. 11

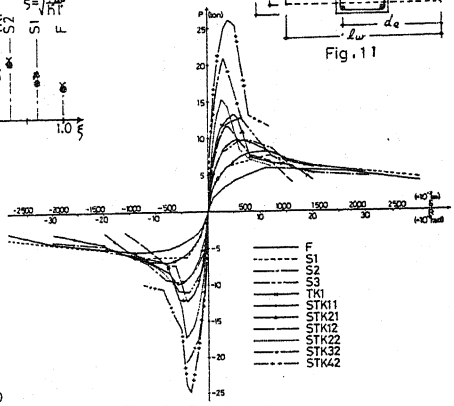

Fig. 10 Envelope Curves